Journal of Thermal Analysis and Calorimetry (2021) 146:1853–1864
https://doi.org/10.1007/s10973-020-10091-5

Simulation study of solar-source heat pump system with sensible energy storage

Kadir Bakirci[1] · Bedri Yuksel[2]

Received: 14 March 2020 / Accepted: 16 July 2020 / Published online: 31 August 2020

Abstract

A simulation study of the solar-source heat pump (SSHP) system that consists of solar collector group, heat exchanger (water-to-water), energy storage tank, heat pump with vapor compression and circulating pumps is carried out. The performance of the designed system is investigated both experimentally and theoretically. The performance of coefficient of the heat pump in the refrigerant circuit (COP) and whole system (COPS) is computed in the range of 3.1–4.2 and 2.3–3.3, respectively. The sensible energy stored system used of the water as storage matter is theoretically tested for the first time in the cold climate conditions. A simulation model of the energy stored SSHP is also performed, and the simulation results are compared with the experimental conclusion. In average, the differences between the theoretical and experimental values of the COP and COPS are about 8 and 5%, respectively. It is found that the developed model corresponds well with the experimental data.

Keywords Solar energy · Heat pump · Energy storage · Solar-source heat pump · Sensible energy storage

List of symbols

A	Area (m^2)
C	Specific heat (kJ kg^{-1} K^{-1})
I	Instantaneous solar radiation (W m^{-2})
$\dot{m}$	Mass flow (kg s^{-1})
$\dot{Q}$	Heat load (rate) (kW)
T	Temperature (°C)
V	Volume (m^3)
$\dot{W}$	Power (kW)
x	Vapor quality

Greeks

Δ	Difference
η	Efficiency
υ	Specific volume (m^3 kg^{-1})

Subscripts

amb	Ambient
aw	50% antifreeze–water mixture
c	Condenser
cd	Condensation
cl	Collector
cp	Compressor
cwo	Water outlet from condenser
e	Evaporator
ev	Evaporation
ewi	Water inlet from exchanger
i	Inclined plane
l	Liquid
p	Pump
pe	Plate heat exchanger
r	Refrigerant
s	Swept
sat	Saturate
sh	Superheating
sc	Subcooling
t	Tank
w	Water
v	Vapor

Abbreviations

COP	Coefficient of performance for heat pump
COPS	Coefficient of performance for whole system
EST	Energy storage tank
SSHP	Solar-source heat pump

✉ Kadir Bakirci
abakirci@atauni.edu.tr

[1] Department of Mechanical Engineering, Atatürk University, 25240 Erzurum, Turkey

[2] Department of Mechatronics Engineering, Istanbul Gelişim University, 34315 Istanbul, Turkey

Introduction

The solar-source heat pump systems ensure a clean and new way in the heating sector. These systems present important environmental protection and energy saving when compared with the conventional systems. They are rising with the appearances of the energy crisis in the world and the increasing environmental problems. As regards global environmental problems, the emissions of world's carbon dioxide have increased with its energy consumption. Turkey is excessively addicted on external energy resources that influence the economy, and harmful emissions in environmental are becoming an important problem in the country.

Heat pumps supply heating with renewable energy from the natural sources in higher quality. These systems are appropriate systems to produce heat in an environmentally responsible and to save on heating costs. Only electrical energy is necessary to run them. This makes heat pumps it free of fossil-based fuels, and actively contributes toward decreasing environmentally damaging emissions.

Many countries have undertaken a leading role in reducing of harmful greenhouse emissions. In this respect, clean and new energy sources seem to be one of the most important ways for sustainable energy in the country. Geographic location of Turkey has various benefits for common utilization of these clean and new energy resources. The energy requirement at low temperature of a heat pump provides it an important advantage according to other heating with its low cost.

The performances of heat pumps have been examined experimentally and theoretically in open literature [1–8]. Tagliafico et al. [7] performed a study on energy saving of the SSHP systems for heating the water of swimming pool. The calculations in here were carried out for thermal load and operating temperatures with the climatic data of all Municipalities in Italian. Yumrutas and Kaska [8] made a design of a SSHP for residence heating and examined its thermal performance. The effects of several operating parameters and climatic conditions on the performance of the system were examined. The COP value was approximately 2.5 in a cloudy day, while it is approximately 3.5 in a sunny day.

In addition, to estimate the performance of solar energy systems, the methods such as particle swarm optimization (PSO), artificial neural network (ANN) and genetic algorithm (GA) are used in the literature [9–11]. Paradeshi et al. [9] carried out on the study the thermodynamic analysis of the direct-expansion solar-source heat pump system under the metrological conditions of India. They established ANN integrated with GA network model to forecast the performance of a direct-expansion solar-source heat pump system. Mohanraj et al. [10] presented the suitability of artificial neural network (ANN) to predict the performance of a direct expansion solar-source heat pump.

Also, the simulation studies in the systems of solar heat pump are commonly used in the literature [12–15]. Ammar et al. [12] reported the energy and exergy performance of a photovoltaic/thermal solar-source heat pump system with different solar radiation amount. They established mathematically models for each component of the heat pump system and the parts of the photovoltaic/thermal evaporator/collector. The COP value increased with increase in solar radiation amount, and the average COP value was found to be 6.14. Krakow and Lin [14] performed a simulation study to examine the performance of the heat pumps running with different sources. The simulation carried out in the conditions of cold climate of the country. The developed model program based on experimental investigations and determined the steady-state performance of a heat pump system. Elasfouri and Hawas [15] improved a simple model for the simulation of a solar energy system. The study was performed for a hot water system in Benghazi, Libya, and the obtained results showed the effects of several parameters to the system performance and the ability of the model.

Paradeshi et al. [16] experimentally investigated the exergy performance of direct-expansion solar-source heat pump systems. The exergy destructions of the systems working with R22 and R433A were calculated to be 1.36 and 1.25 kW, respectively. The artificial neural network model was developed to simulate the performance of this system. James et al. [17] reviewed the thermal analyses of heat pump systems with photovoltaic-thermal collectors. They described the energy equations used for modeling the photovoltaic-thermal collectors.

The assessments of the environmental impact and life cycle cost of solar-source heat pump systems are required to evaluate by comparing with alternative heating modes [18]. The initial costs of the heat pumps are higher, but they have lower operating, maintenance and life cycle costs than most conventional systems. Bakirci and Yuksel [6] examined the impacts of the environmental and economical of the solar-source heat pump system carried out simulation study in this paper. The CO_2 ratios of various alternative systems for 18,900 kWh year^{-1} in residential heating were calculated. It was stated that the systems with coal, fuel–oil, LPG and natural gas released to environment the CO_2 emission in the values of 9779, 6338, 4961 and 5051 kg year^{-1}, respectively, while the CO_2 emission of the heat pump system is zero when the electric energy is produced by green energy resources. In other respects, It was expressed that the

payback period of the heat pump system (for COPS = 2.7) was absent due to relatively low price of natural gas, while the payback periods of the heat pump system according to the LPG, electric and fuel oil were 1.4, 2.9 and 3.9 years, respectively.

In this study, the system's performance we proposed is examined experimentally and theoretically. The sensible energy stored system used of the water as storage matter is theoretically tested for the first time in the cold climate conditions of the country. The variations of the working fluid (antifreeze–water) temperature in the solar collectors, the water temperature in the EST, the COP and the COPS during the day are investigated. Besides, the yield of solar collector group and the heat transfer rate in the condenser unit of the system are calculated. The simulation program written in MATLAB [19] is also utilized to analyze the experimental results and the performance of the SSHP.

Working principle of SSHP

As indicated in Fig. 1, the system that the experimental measurements are received consists of three basic circuits which contains to solar collector group, heat pump and EST. In the experimental system, the working fluid that leaves from the collector group firstly arrives to the EST where a part of the thermal energy is stored. It is then utilized by the evaporator of the system as a heat source and is dispatched to the collector group. At nights, the water in lower temperature leaving from the evaporator goes to

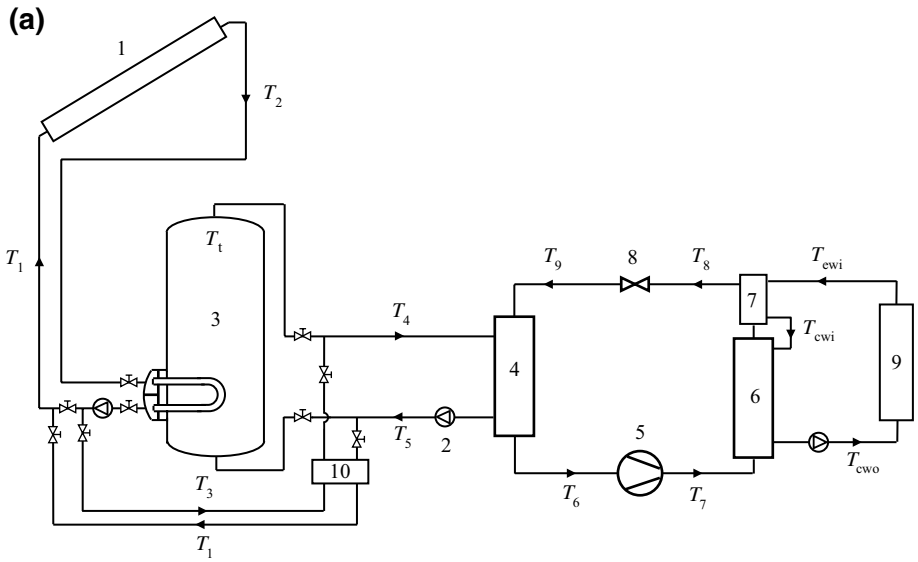

1. Solar collector
2. Circulating pump
3. Energy storage tank
4. Evaporator
5. Compressor
6. Condenser
7. Prior heating and sub-cooling exchanger
8. Expansion valve
9. Radiator
10. Plate-heat exchanger

Fig. 1 SSHP system with energy storage, **a** the temperatures used in calculations, **b** the photograph of the experimental setup

(b)

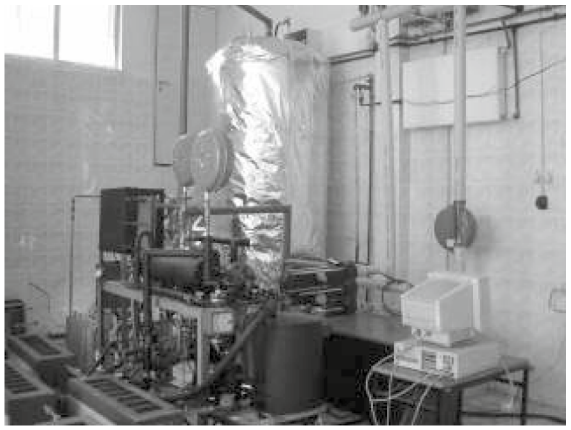

the EST and it receives energy from the EST instead of the collector group.

Benefits of the heat pumps

The SSHP systems supply a clean and new manner of heating in buildings. These systems have great number of environmental advantages when compared to the other existing systems. For this reason, they can be utilized to minimize harmful environmental effects. They present an influential way to supply cooling and heating in many industrial and domestic applications so that they can utilize renewable clean heat resources in the world.

Computations in experimental system

The values of the COP can be determined as:

$$\mathrm{COP} = \frac{\dot{m}_c C_w (T_{cwo} - T_{ewi})}{\dot{W}_{cp}} \tag{1}$$

The values of the COPS are computed as below:

$$\mathrm{COPS} = \frac{\dot{m}_c C_w (T_{cwo} - T_{ewi})}{\dot{W}_{cp} + \dot{W}_{\Sigma p}} \tag{2}$$

where $\dot{W}_{cp}$ is the power of the compressor and $\dot{W}_{\Sigma p}$ is the total power of the circulation pumps.

Also the instantaneous yields of the collector group can be calculated as:

$$\eta_{cl} = \frac{\dot{Q}_{cl}}{A_{cl} I_i} \tag{3}$$

where $\dot{Q}_{cl}$ is the useable heat load ensured by the solar collector group, and it can be computed as:

$$\dot{Q}_{cl} = \dot{m}_{cl} C_{aw} (T_2 - T_1) \tag{4}$$

where T_1 is the inlet temperatures of the working fluid to the collector group and T_2 is the outlet temperature from the solar collector of the working fluid (antifreeze–water mixture). Also, the useable heat load in the condenser unit (including prior heating and subcooling exchanger) is calculated from the equation in following:

$$\dot{Q}_c = \dot{m}_c C_w \left(T_{cwo} - T_{ewi}\right). \tag{5}$$

Theoretical calculations

A theoretical model of the experimental SSHP system is developed, where its details are explained below. The system consists of three basic parts: solar collector group, heat pump and EST (Fig. 1). In the developed dynamic simulation model, some acceptances are carried out to simplify the numerical calculations, which are given as follows:

- The slope angle of the solar collector group with the horizontal plane is 50°.
- The inlet temperature to the collectors of heat transfer fluid (T_1) is taken as an initial parameter according to experimental data.
- Overall heat loss coefficient of the solar collector group (U_{cl}) is 7 W(m^2 °C)$^{-1}$.
- The heat losses in the EST are neglected since the tank is well insulated.
- The pressure drops in the evaporator and condenser are neglected, and the refrigerant is accepted to be saturated vapor at the outlet of the heat exchanger.
- The compression process in the compressor is considered as isentropic.
- The expansion in the expansion valve is considered isenthalpic.
- Superheating is taken to be a function of evaporator water inlet temperature.
- Subcooling is assumed to be 3 °C.
- Power of the circulation pumps is taken as a constant (the power values for antifreeze–water circulation pump and a water circulation pump are 0.155 and 0.137 kW, respectively).
- Working fluid is selected as R-134a (the thermodynamic and environmental properties of R-134a are given in Table 1).

The model equations used in the simulation are given in the following:

Collector

The energy equation of the collector group can be defined as:

$$\dot{Q}_{cl} = F_R A_{cl} \left[I_i (\tau\alpha) - U_{cl} \left(T_1 - T_{amb}\right) \right] = \dot{m}_{cl} C_{aw} \left(T_2 - T_1\right) \tag{6}$$

and, the temperature of T_2 is calculated as:

Table 1 Thermodynamic and environmental properties of R-134a [20]

Nos.	Properties	R-134a
1	Boiling point at 101.3 kPa/°C	− 26.1
2	Critical temperature/°C	101.1
3	Critical pressure/MPa	4.06
4	Ozone depletion potential	0
5	Global warming potential	1300

$$T_2 = T_1 + \frac{A_{cl}F_R}{\dot{m}_{cl}C_{aw}}\left[I_i(\tau\alpha) - U_{cl}\left(T_1 - T_{amb}\right)\right] \quad (7)$$

The F_R, U_{cl}, I_i and T_{amb} values in Eq. (6) are calculated by means of the equations given in the open literature [21–23]. Also, the solar radiation values of the clear sky on horizontal plane can be computed by the methods given in the literature.

Energy storage tank (EST)

The thermal energy received from the solar by the collector group is stored to be sensible heat in water in here. In the model of the utterly mixed tank, it is presumed that the working fluid (water) temperature in the EST outlet is in the mean temperature of the EST, while in the situation of the stratified simulation, no mixing takes place among layers in the EST. In according to some acceptances, a functional relation may be contacted between the mean temperature of the tank and the outlet temperature from the EST of water. The energy equation of the tank can be stated as follows:

$$\dot{Q}_t = \dot{m}_{cl}C_{aw}(T_2 - T_3) = M_tC_w\frac{dT_t}{dt} \quad (8)$$

and, if Eq. (8) is written again according to effectiveness (ε_t) of the heat exchanger in the EST tank, it can be expressed as:

$$\dot{Q}_t = \dot{m}_{cl}C_{aw}\varepsilon_t(T_2 - T_t) = M_tC_w\frac{dT_t}{dt} \quad (9)$$

where the values of ε_t is found from the experimental data and expressed as:

$$\varepsilon_t = \frac{T_2 - T_3}{T_2 - T_t} \quad (10)$$

Then, the top region temperature of the EST (T_t) can be calculated as Kilic and Ozturk [24]:

$$T_t = \frac{1}{1 + W_t}\left[W_tT_{ti} + T_2\right] \quad (11)$$

where the value of T_{ti} is the initial temperature of the EST and is measured before the experiment starts. The value of W_t can be calculated as follows:

$$W_t = \frac{M_tC_w}{\dot{m}_{cl}C_{aw}\varepsilon_t\Delta t} \quad (12)$$

where the term of Δt is the time interval of the experimental measurements and it is 15 min. Thus, the temperature of T_3 can be calculated from Eq. (8). The temperature of T_4 is given by $T_4 = f(T_3)$.

Plate-heat exchanger

In this study, the working fluid coming from the collector group firstly arrives to the EST where a part of its energy gives, and then, it is utilized to be a heat energy source by the evaporator passing through the heat exchanger. In this way, the heat pump is supplied heat source during the day. The heat extracted by the heat exchanger can be computed as below:

$$\dot{Q}_{pe} = \dot{m}_{cl}C_{aw}(T_3 - T_1) = \dot{m}_eC_w(T_4 - T_5) = \dot{m}_eC_w\varepsilon_{pe}(T_3 - T_5) \quad (13)$$

where ε_{pe} is the effectiveness of the heat exchanger, and it is calculated by the ε-NTU relation written for the heat exchanger. The inlet temperature of the heat carrier fluid to the heat exchanger (T_5) is calculated from the effectiveness of the plate-heat exchanger as follows:

$$T_5 = \left(\varepsilon_{pe}T_3 - T_4\right)/\left(\varepsilon_{pe} - 1\right). \quad (14)$$

Evaporator

The cooling-to-heating process in the evaporator is managed by the four equations involving the energy balance between refrigerant and heat transfer fluid [Eqs. (15) and (16)], the refrigerant-fluid heat transfer equation (Eq. 17) and the effectiveness of the evaporator (Eq. 18). Therefore, the evaporator equations are given as follows:

$$\dot{Q}_e = \dot{m}_r\left[(1 - x_9)h_{lve} + (h_6 - h_v(T_{ev}))\right] \quad (15)$$

$$\dot{Q}_e = \dot{m}_eC_w(T_4 - T_5) \quad (16)$$

$$\dot{Q}_e = \dot{m}_eC_w\varepsilon_e(T_4 - T_{ev}) \quad (17)$$

$$\varepsilon_e = \frac{(T_4 - T_5)}{(T_4 - T_{ev})}. \quad (18)$$

Compressor

In the modeling of this equipment, it is assumed that compression in the compressor traces an isentropic process of constant index (k). The ratio of the specific volume at the output of the compressor to the specific volume at the input can be written as:

$$v_7 = v_6\left(P_{ev}/P_{cd}\right)^{1/k} \quad (19)$$

The mass flow rate of the refrigerant is calculated by equation in the following:

$$\dot{m}_r = \frac{nV_s}{v_6} \tag{20}$$

where n is the rotation speed, V_s is the constant swept volume, not known a priori (or taken in fictitious value as a model parameter), and the specific volume at the compressor inlet has to be computed taking into account the heating-up [25].

The power of the compressor can be calculated as follows:

$$\dot{W}_{cp} = \dot{m}_r\left(h_7 - h_6\right). \tag{21}$$

Condenser

The condenser follows the evaporator model, and the equations in the condenser unit are given by:

$$\dot{Q}_c = \dot{m}_r(h_7 - h_8) \tag{22}$$

$$\dot{Q}_c = \dot{m}_c C_w(T_{cwo} - T_{ewi}) \tag{23}$$

$$\dot{Q}_c = \dot{m}_r\left[Cp_{rvc}\left(T_7 - T_{cd}\right) + h_{lvc} + Cp_{rlc}\left(T_{cd} - T_8\right)\right] \tag{24}$$

$$\dot{Q}_c = \dot{m}_c C_w \varepsilon_c (T_7 - T_{ewi}) \tag{25}$$

$$\varepsilon_c = \frac{(T_{cwo} - T_{ewi})}{(T_7 - T_{ewi})}. \tag{26}$$

Expansion valve

The enthalpy of the refrigerant remains constant. The equations of the expansion valve are written as follows:

$$h_8 = h_9 \tag{27}$$

$$h_l(T_8) = h_l(T_{ev}) + x_9 h_{lve}(T_{ev}) \tag{28}$$

$$x_9 = 1 + \frac{Cp_{rve}\Delta T_{sh}}{h_{lve}} - \frac{\dot{m}_e C_w \varepsilon_e (T_4 - T_{ev})}{\dot{m}_r h_{lve}}. \tag{29}$$

Property equations of refrigerant

The related property equations of the refrigerant can be written as follows:

$$P_{ev} = P_{sat}\left(T_{ev}\right) \tag{30}$$

$$P_{cd} = P_{sat}\left(T_{cd}\right) \tag{31}$$

$$v_6 = v_v\left(T_6, P_{ev}\right) \tag{32}$$

$$v_7 = v_v\left(T_7, P_{cd}\right) \tag{33}$$

$$Cp_{rl} = Cp_{rl}\left(T_{ev}\right) \tag{34}$$

$$Cp_{rv} = Cp_{rv}\left(T_{cd}\right) \tag{35}$$

$$h_6 = h_v\left(T_6, P_{ev}\right) \tag{36}$$

$$h_7 = h_v\left(T_7, P_{cd}\right) \tag{37}$$

$$h_{lve} = h_{lv}\left(T_{ev}\right) \tag{38}$$

$$h_{lvc} = h_{lv}\left(T_{cd}\right) \tag{39}$$

$$h_8 = h_l(T_8) \tag{40}$$

$$h_9 = h_{9l} + x_9 h_{lve}(T_{ev}) \tag{41}$$

$$h_{9l} = h_l(T_{ev}) \tag{42}$$

Thus, Eqs. (6)–(42) have been generated. The equivalent 30 unknown variables have been selected as follows:

Collector: $\dot{Q}_{cl}$, T_2
Storage tank: $\dot{Q}_t$, W_t, T_3, T_4
Plate-heat exchanger: $\dot{Q}_{pe}$, T_5
Evaporator: $\dot{Q}_e$, T_{ev}, x_9, h_{lve}
Compressor: v_6, v_7, P_{ev}, P_{cd}, $\dot{m}_r$, h_6, h_7, T_6, T_7
Condenser: $\dot{Q}_c$, Cp_{rl}, Cp_{rv}, T_{cd}, T_8, T_{cwo}, h_{lvc}
Expansion valve: h_8, h_9

Input data

Collector: A_{cl}, $\dot{m}_{cl}$, $(\tau\alpha)$, F_R, U_{cl}, C_{aw},
Storage tank: M_t, Δt, C_w, ε_t,
Plate-heat exchanger: $\dot{m}_e$, ε_{pe}
Evaporator: ε_e
Compressor: k, n, V_s
Condenser: $\dot{m}_c$, ε_c, ΔT_{sc}

Solution

The equation system of (6)–(42) can be decreased, by direct placement, to three nonlinear equations in the function of T_{ev}, T_{cd} and T_7 as the independent variables. The temperatures in the characteristic points of heat pump indicated in

Fig. 1 are obtained by the solution of these three nonlinear equations as follows [1]:

$$v_7 - v_6\left(P_{ev}/P_{cd}\right)^{1/k} = F\left(T_{ev}, T_{cd}, T_7\right) = 0 \tag{43}$$

$$h_l(T_8) - h_l(T_{ev}) - x_9 h_{lve}(T_{ev}) = F\left(T_{ev}, T_{cd}, T_7\right) = 0 \tag{44}$$

$$\dot{m}_c C_w \varepsilon_c (T_7 - T_{ewi}) - \dot{m}_r (h_7 - h_6) - \dot{m}_e C_w \varepsilon_e (T_4 - T_{ev}) = F\left(T_{ev}, T_{cd}, T_7\right) = 0 \tag{45}$$

In this study, the temperature of evaporation (T_{ev}), condensation (T_{cd}) and outlet from the compressor of refrigerant (T_7) are found using a computer program written in MATLAB [19]. Thus, the calculations related to the heat pump can be performed using the temperatures of T_{ev}, T_{cd} and T_7. The temperatures T_6 and T_8 are defined as follows:

$$T_6 = T_{ev} + \Delta T_{sh} \tag{46}$$

$$T_8 = T_{cd} - \Delta T_{sc} \tag{47}$$

where ΔT_{sh} is the temperature of superheating and found from the function of $\Delta T_{sh} = f(T_4)$, and ΔT_{sc} is the temperature of subcooling and taken as a constant value of $\Delta T_{sc} = 3$. The temperature of T_{ewi} in Eq. (45) is the front heat exchanger inlet temperature of water and found from the function of $T_{ewi} = f(T_4)$.

Uncertainty analysis

In this study, the solar radiation values, temperatures, pressures, flow rates and average electrical power inputs are determined by various measuring instruments [23]. The uncertainty analysis for the experimental measurement devices is carried out by a calculation method suggested by Holman [26]

$$W_R = \left[\left(\frac{\partial R}{\partial x_1} w_1\right)^2 + \left(\frac{\partial R}{\partial x_2} w_2\right)^2 + \cdots + \left(\frac{\partial R}{\partial x_n} w_n\right)^2\right]^{1/2} \tag{48}$$

where the result R is a given function of the independent variables $x_1, x_2, \ldots, x_n$ and $w_1, w_2, \ldots, w_n$ are the uncertainties in the independent variables.

In the experimental measurements, the uncertainties are predicted to be ± 1.0% for the temperatures of all working fluids (± 0.5 °C for 50 °C), ± 4.0% for solar radiation (± 20 W m^{-2} for 500 W m^{-2}) and ± 2.1% for the pressures read from the manometers (± 0.042 MPa for 1.98 MPa). The uncertainties for the power inputs of the compressor (± 0.011 kW for 1.058 kW) and the pumps (± 0.004 kW for 0.137 kW, in a water circulation pump) are ± 1.0% and ± 3.0%, respectively. The uncertainties in the flow meters for working fluids of water (such as ± 0.007 kg s^{-1} for 0.125 kg s^{-1} in evaporator), refrigerant (± 0.0004 kg s^{-1} for 0.016 kg s^{-1}) and ethylene glycol solution (± 0.003 kg s^{-1} for 0.180 kg s^{-1}) are forecasted to be ± 5.2%, ± 2.2% and ± 1.8%, respectively. It is supposed that the uncertainties in the reading from the thermodynamics tables are ± 0.2%. The uncertainties for the heat loads of the condenser and the evaporator are ± 5.3%. The uncertainty associated with the instantaneous collector efficiency is ± 4.75%. The uncertainties for the COP and COPS are approximately ± 5.4.

Model performance

In the literature, various statistical methods are used to test models. In the present study, the statistical evaluation of the simulation model is tested by the following statistical methods: the mean bias error (MBE), root mean square error (RMSE) and correlation coefficient (r) [27, 28].

Table 2 Inputs for MATLAB computer simulation

Data	Value
Month and day of the year (for example, March 8)	3 and 8
Time interval of simulation (Δt)/s	900
Initial temperature (T_1)/°C	18.5
A_{cl}/m^2	19.69
$\dot{m}_{cl}$/kg s^{-1}	0.180
C_{aw}/J kg^{-1} K^{-1}	3349
C_w/J kg^{-1} K^{-1}	4180
U_{cl}/W m^{-2} K	7.0
$\tau\alpha$	0.77
F_R	0.81
M_t/kg	2000
ε_t	0.601
ε_{pe}	0.293
ε_e	0.254
ε_c	0.225
Time of day/h	09:00–24:00
$\dot{m}_e$/kg s^{-1}	0.125
$\dot{m}_c$/kg s^{-1}	0.167
Isentropic exponent/k	1.03
Revolution number of compressor (N)/rev s^{-1}	48.33
Displacement volume of compressor (V_s)/m^3	5.34
Subcooling (ΔT_{sc})/°C	3.0

Table 3 Meteorological data in average and technical features of the system

Location: Province of Erzurum, Turkey (latitude 39.55° N; longitude 41.15° E)	
Yearly average values	
Temperature of outdoor/°C	4.7
Temperature of minimum outdoor/°C	−2.8
Temperature of maximum outdoor/°C	12.2
Value of relative humidity/%	64.6
Daily solar radiation/MJ m^{-2} day^{-1}	15.6
Value of wind velocity/m s^{-1}	2.7
Main element information	Technical specification
Pyranometer	
Measuring range/W m^{-2}	0–1800
Resolution and units/W m^{-2}	1
Collector	
Type (copper tube and fin)	Flat-plate
Glass number	Single
Collector area/m^2	1.64
Collector number	12
Capacity/L	3.5
Water-ethylene glycol mass flow rate in collectors/L h^{-1}	600
Cylindrical energy storage tank	
Volume of water in store/L	2000
Wall thickness/mm	7
Diameter/mm	1000
Surface area of serpentine/m^2	4
Flowmeters	
Measuring range (water–ethylene glycol)/L h^{-1}	150–1500
Measuring range (refrigerant)/L h^{-1}	25–250
Measuring range (water in condenser and evaporator)/L min^{-1}	5–35
Circulation pumps	
Type (three-stage variable speed)/V Hz^{-1}	220–240/1–50
Heat pump	
Compressor type (hermetic-scroll)/V Hz^{-1}	220–240/1–50
Evaporator and condenser type	Shall-and-tube
Compressor displacement/m^3 h^{-1}	5.34
Compressor rotation speed/rpm	2900
Water mass flow rate in evaporator/L h^{-1}	450
Water mass flow rate in condenser/L h^{-1}	600
Refrigerant type	R-134a

Results and discussion

The energy analysis of the sensible heat energy stored SSHP system in cold climate conditions of Turkey is carried out experimentally and theoretically. In the study, a quasi-steady

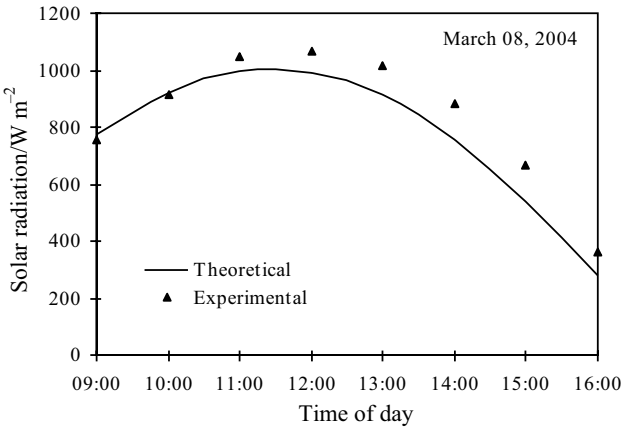

Fig. 2 Values of theoretical and experimental of instantaneous solar radiation during the day

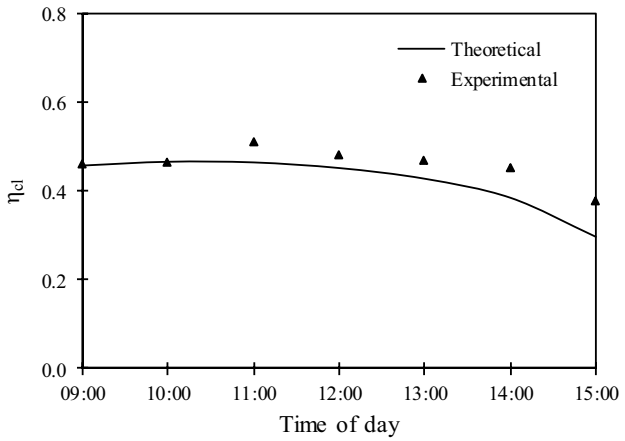

Fig. 3 Values of theoretical and experimental of solar collector group's efficiency during the day

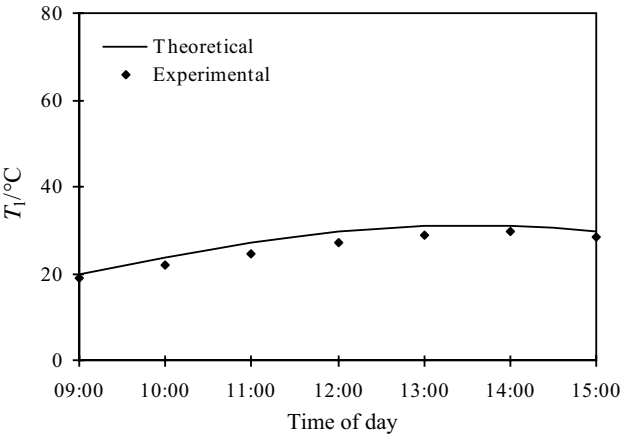

Fig. 4 Values of theoretical and experimental of T_1 during the day

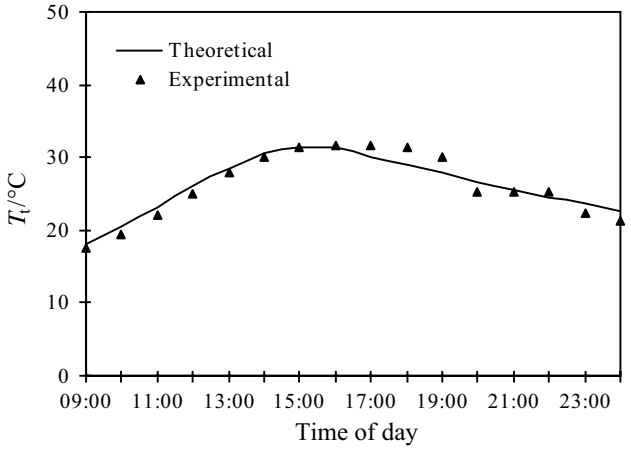

Fig. 5 Values of theoretical and experimental of T_t in the EST during the day

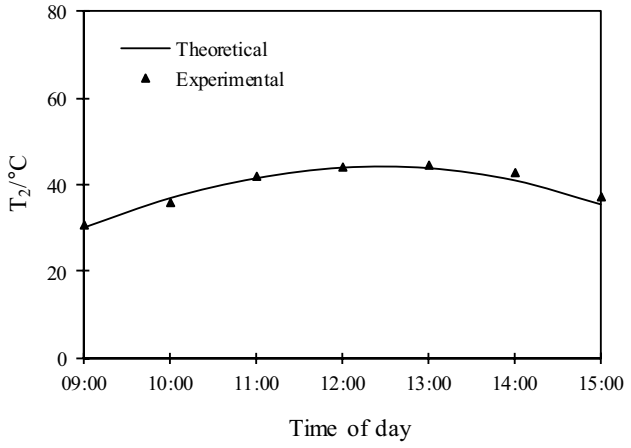

Fig. 6 Values of theoretical and experimental of T_2 during the day

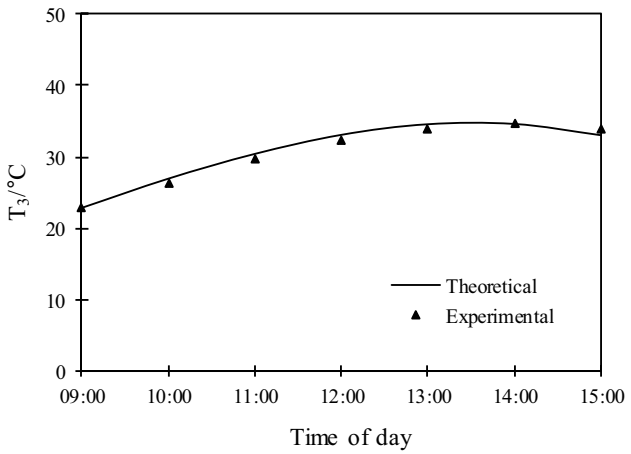

Fig. 7 Values of theoretical and experimental of T_3 during the day

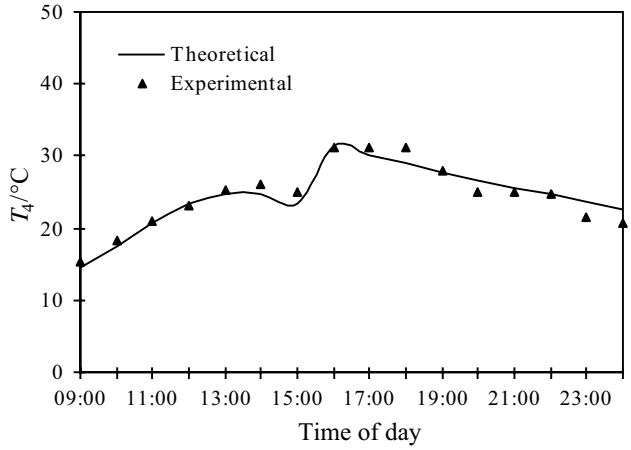

Fig. 8 Values of theoretical and experimental of T_4 during the day

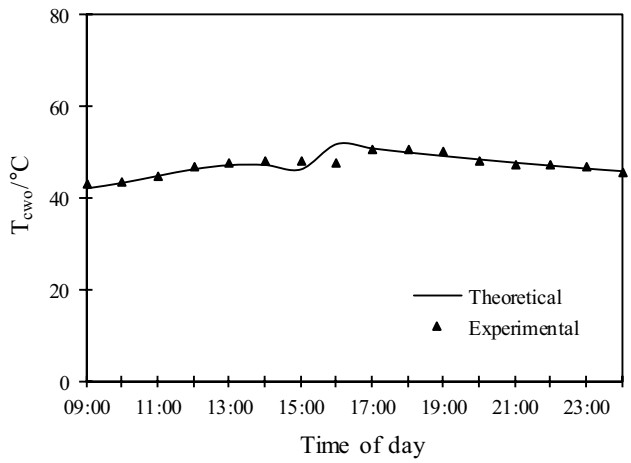

Fig. 9 Values of theoretical and experimental of T_{cwo} during the day

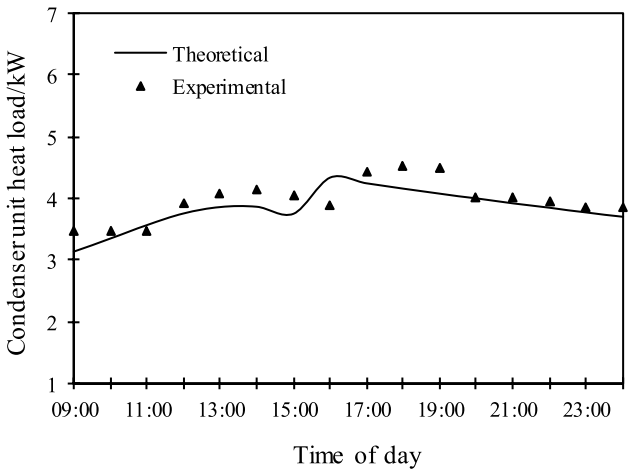

Fig. 10 Values of theoretical and experimental of the heat loads taken from the condenser unit during the day

state is taken place so that the experiment results are obtained under clear sky conditions.

The complication of the energy analysis of the SSHP makes a feasible method to the use of only computer simulations for designating to the system's energy performance and its dynamics. Although the existing simulations are developed to research aims, it is very complex and overpriced for designers to use them. Therefore, there is necessity to simple simulations which can be utilized on computers. Moreover, these models allow to be examined of the dynamic behavior of the considered system and the changes in the configuration and parameters of the system. In the study, the theoretical and experimental results obtained throughout the day are given according to local time.

In here, a simplified simulation model is developed. This model is utilized in order to simulate the SSHP system in domestic heating applications for Erzurum province having cold climate in Turkey. Table 2 tabulates the required inputs for the MATLAB simulation program. The climatic data for the related region and the technical specifications of the system are given in Table 3.

The values of theoretical and experimental solar radiation, I_i (W m^{-2}), during the day are presented in Fig. 2. It is seen from Fig. 2 that the values of the global solar radiation range from 277 to 1067 W m^{-2}.

The theoretical and experimental collector group's efficiency during the day is illustrated in Fig. 3. In average, the theoretical and experimental efficiency values of the collector group are 0.42 and 0.46, respectively. The values of the theoretical and experimental of T_1, T_t, T_2, T_3 and T_4 during the day are shown in Figs. 4, 5, 6, 7 and 8, respectively. The temperature values of the T_1, T_t, T_2, T_3 and T_4 change approximately between 19–31, 18–32, 30–45, 23–35 and 15–31 °C, respectively. The values of theoretical and experimental of T_{cwo} during the day are given in Fig. 9. The values of the T_{cwo} change between 42 and 52 °C nearly. The conclusions of the theoretical and the experimental of the heat loads taken from the condenser unit ($\dot{Q}_c$) throughout the day are given in Fig. 10. The average values of the theoretical and experimental heat loads taken from the condenser unit are about 3.84 and 3.96 kW, respectively. In here, the difference between the theoretical and experimental values is about 3%. Figures 11 and 12 demonstrate to the COP and the COPS of the theoretical and the experimental versus time of day, respectively. While the values of the experimental COP are in the range of 3.1–4.1 and their average is 3.7, the values of the theoretical COP are in the range of 4.0–4.2 and their average is 4.1. On the other part, while the values of the experimental COPS are in the range of 2.3–3.3 and their average is 2.8, the values of the theoretical COPS are in the range of 2.6–3.3 and their average

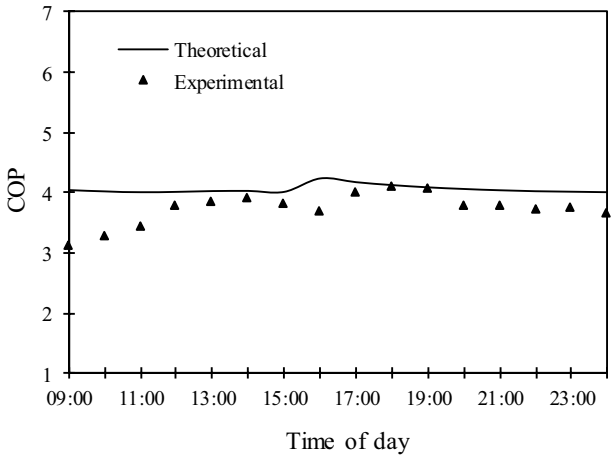

Fig. 11 COP values of theoretical and experimental during the day

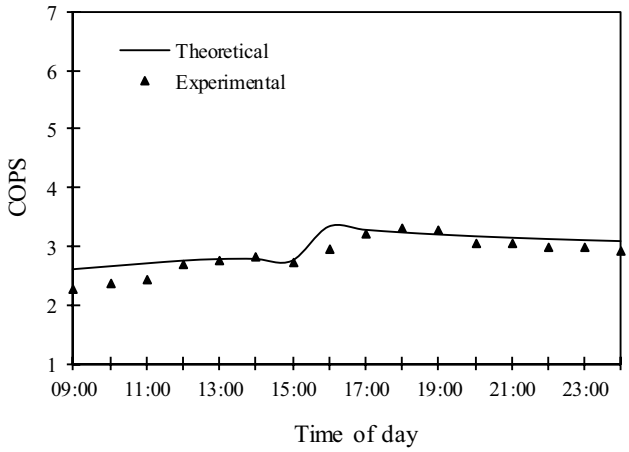

Fig. 12 COPS values of theoretical and experimental during the day

is 3.0. In average, the differences between the theoretical and experimental values of the COP and COPS are about 8 and 5%, respectively. It is seen that the simulation and the test results are in good agreement. The EST is used approximately at 16:00 local time. The source temperature supplied to the heat pump suddenly rises about 8–9 °C when the EST is used. Meantime, while the effect of the sudden increase in the source temperature on the results is seen immediately in theoretical calculations, it takes some time to be seen in experimental results. Therefore, some deviation occurs in the theoretical and experimental results at local times when the temperature suddenly changes.

The values of MBE, RMSE and r for simulation model are presented in Table 4. It is seen that the model results are closer to experimental values with the correlation coefficient between 0.687 and 0.988. These results

Table 4 Values of MBE, RMSE and r for simulation model

Statistics	T_1	T_t	T_2	T_3	T_4	T_{cwo}	$\dot{Q}_c$	COPS
MBE	1.679	0.112	−0.593	0.364	−0.107	0.118	−0.122	0.145
RMSE	1.777	1.220	1.055	0.646	1.192	1.261	0.230	0.198
r	0.880	0.963	0.976	0.988	0.963	0.814	0.687	0.751

confirm that developed simulation model gives satisfactory results.

Conclusions

In this study, a simulation program is developed to examine a sensible heat energy stored solar-source heat pump system. The some system parameters are obtained from experimental data. The following results can be exhibited from this study:

- The conclusions of the theoretical and the experimental of the temperature of T_{cwo} indicate that it ranges from 42.1 to 52.0 °C and from 42.8 to 50.5 °C, respectively. In average, the difference between the theoretical and experimental T_{cwo} is about 0.3%.
- The maximum theoretical and experimental temperatures (T_t) in the energy storage tank are 31.5 °C and 31.7 °C, respectively. In here, the difference between the theoretical and experimental T_t is about 0.6%.
- The average values of the theoretical and experimental heat loads taken from the condenser unit are about 3.84 and 3.96 kW, respectively. In average, the difference between the theoretical and experimental values is about 3%.
- The values of the experimental and theoretical COP in average are 3.7 and 4.1, while the values of the experimental and theoretical COPS in average are 2.8 and 3.0, respectively. In average, the differences between the theoretical and experimental values of the COP and COPS are about 8 and 5%, respectively.
- The simulation program improved in here can be utilized to investigate how the performance of a SSHP system changes due to different operating conditions and system parameters. It is concluded that the values of the simulation are in good agreement with the test results. It is seen that the model results are closer to experimental values with the correlation coefficient of 0.988 for T_3.

Acknowledgements The authors thank to the Atatürk University Research Fund for their support for the establishment of the system in which the experimental results are received.

References

1. Herbas TB, Berlinck EC, Uriu CAT, Marques RP, Parise JAR. Steady-state simulation of vapour-compression heat pumps. Int J Energy Res. 1993;17:801–16.
2. Chyng JP, Lee CP, Huang BJ. Performance analysis of a solar-assisted heat pump water heater. Sol Energy. 2003;74:33–44.
3. Qi Q, Deng S, Jiang Y. A simulation study on a solar heat pump heating system with seasonal latent heat storage. Sol Energy. 2008;82:669–75.
4. Li YW, Wang RZ, Wu JY, Xu YX. Experimental performance analysis and optimization of a direct expansion solar-assisted heat pump water heater. Energy. 2007;32:1361–74.
5. Mohanraj M, Jayaraj S, Muraleedharan C. A comparison of the performance of a direct expansion solar assisted heat pump working with R22 and a mixture of R407C–liquefied petroleum gas. Proc Inst Mec Eng Part A J Power Energy. 2009;223:821–33.
6. Bakirci K, Yuksel B. Experimental thermal performance of a solar source heat pump system for residential heating in cold climate region. Appl Therm Eng. 2011;31:1508–18.
7. Tagliafico LA, Scarpa F, Tagliafico G, Valsuani F. An approach to energy saving assessment of solar assisted heat pumps for swimming pool water heating. Energy Build. 2012;55:833–40.
8. Yumrutas R, Kaska O. Experimental investigation of thermal performance of a solar assisted heat pump system with an energy storage. Int J Energy Res. 2004;28:163–75.
9. Paradeshi L, Srinivas M, Jayaraj S. Thermodynamic analysis of a direct expansion solar-assisted heat pump system working with R290 as a drop-in substitute for R22. J Therm Anal Calorim. 2019;136:63–78.
10. Mohanraj M, Jayaraj S, Muraleedharan C. Performance prediction of a direct expansion solar assisted heat pump using artificial neural networks. Appl Energy. 2009;86(1):1442–9.
11. Mohanraj M, Jayaraj S, Muraleedharan C. Applications of artificial neural networks for refrigeration, air-conditioning and heat pump systems A review. Renew Sustain Energy Rev. 2012;16(1):1340–58.
12. Ammar AA, Sopian K, Alghoul MA, Elhub B, Elbreki AM. Performance study on photovoltaic/thermal solar-assisted heat pump system. J Therm Anal Calorim. 2019;136:79–87.
13. Kaygusuz K. Experimental and theoretical investigation of a solar heating system with heat pump. Renew Energy. 2000;21:79–102.
14. Krakow KI, Lin S. A computer model for the simulation of multiple source heat pump performance. ASHRAE Trans. 1983;89:590–616.
15. Elasfouri AS, Hawas MM. A simplified model for simulating solar thermal systems. Energy Convers Manag. 1987;27:1–10.
16. Paradeshi L, Mohanraj M, Srinivas M, Jayaraj S. Exergy analysis of direct-expansion solar-assisted heat pumps working with R22 and R433A. J Therm Anal Calorim. 2018;134:2223–37.
17. James A, Mohanraj M, Srinivas M, Jayaraj S. Thermal analysis of heat pump systems using photovoltaic-thermal collectors: a review. J Therm Anal Calorim. 2020. https://doi.org/10.1007/s10973-020-09431-2.

18. Mohanraj M, Belyayev Y, Jayaraj S, Kaltayev A. Research and developments on solar assisted compression heat pump systems—a comprehensive review (part A: modeling and modifications). Renew Sustain Energy Rev. 2018;83:90–123.
19. MATLAB Reference Guide. The Math Works Inc., Natick; 2008.
20. Devotta S, Waghmare AV, Sawant NN, Domkundwar BM. Alternatives to HCFC-22 for air conditioners. Appl Therm Eng. 2001;21:703–15.
21. Duffie JA, Beckman WA. Solar engineering of thermal processes. 2nd ed. New York: Wiley; 1991.
22. Howell JR, Bannerot RB, Vliet GC. Solar-thermal energy system. New York: McGraw-Hill; 1982.
23. Bakirci K. Experimental and theoretical investigation of solar assisted and energy stored heat pump system in the province of Erzurum. Ph.D. thesis, Erzurum: Atatürk University; 2004 (**in Turkish**).
24. Kilic A, Ozturk A. Solar Energy. Istanbul: Kipas Distribution; 1983 **(in Turkish)**.
25. Winandy EL, Saavedra O, Lebrun J. Experimental analysis and simplified modelling of a hermetic scroll refrigeration compressor. Appl Therm Eng. 2002;22:107–20.
26. Holman IP. Experimental methods for engineers. 6th ed. New York: McGraw-Hill; 1994.
27. Ma CCY, Iqbal M. Statistical comparison of models for estimating solar radiation on inclined surfaces. Sol Energy. 1983;31(3):313–7.
28. Bulut H, Buyukalaca O. Simple model for the generation of daily global solar-radiation data in Turkey. Appl Energy. 2007;84:477–91.